Journal of Integrative Agriculture 2026, 25(9): 3868–3881

KeAi CHINESE ROOTS GLOBAL IMPACT

Available online at ScienceDirect

Journal of Integrative Agriculture

RESEARCH ARTICLE

Fertilizer-N recovery links to SOC stabilization and fractionation in straw-mulched soil: Insights from ^{15}N-tracing and ^{13}C natural abundance

Cong Xu[1, 3, 4], Ziqi Yang[1, 4], Jing Wang[2], Roland Bol[5, 6], Weijie Li[1, 3], Cheng Ji[1, 4], Jie Yuan[1], Lei Wang[1], Dong Liang[1], Hanshen Zhu[1, 4], Jidong Wang[1, 3, 4#], Yongchun Zhang[1, 3], Yuchun Ai[1]

[1] *National Agricultural Experimental Station for Agricultural Environment, Luhe/Institute of Agricultural Resources and Environment, Jiangsu Academy of Agricultural Sciences, Nanjing 210014, China*
[2] *Co-Innovation Center for Sustainable Forestry in Southern China, College of Forestry, Nanjing Forestry University, Nanjing 210037, China*
[3] *College of Resources and Environmental Sciences, Nanjing Agricultural University, Nanjing 210095, China*
[4] *School of the Environment and Safety Engineering, Jiangsu University, Zhenjiang 212013, China*
[5] *Institute of Bio- and Geosciences, Agrosphere (IBG-3), Forschungszentrum Julich GmbH, Julich 52425, Germany*
[6] *School of Natural Sciences, Bangor University, Bangor, Gwynedd, LL57 2UW, United Kingdom*

Highlights

- 1% macroaggregate rise boosts SOC stock by 0.17 Mg ha^{-1} and N recovery by 0.41%.
- Fertilizer-N retention in aggregates is associated with increased SOC stabilization.
- Stable SOC exhibited strongest link to fertilizer-N distribution in soil profile.
- Straw mulching plus reduced N maintained yield and increased fertilizer-N recovery.
- Straw amendment enhanced SOC accumulation and microbial transformation.

Abstract

While straw mulching has the potential to reduce fertilizer-nitrogen (N) losses in intensively managed cropland, how soil organic carbon (SOC) regulates this fate of fertilizer-N at soil aggregate or profile scales remains unresolved. Here, micro-plots were nested within a four-year field experiment to assess fertilizer-N fates and their linkages with SOC fractions and stabilization processes *via* ^{15}N-tracing and ^{13}C natural abundance analyses. Three treatments were included: (i) conventional N application (FN), (ii) reduced N application (RN), and (iii) reduced N with straw mulching (RS). While RN reduced crop yields compared to FN, RS achieved comparable yields and 7.71% higher N recovery efficiency (P<0.05). The δ^{13}C fractionation between aggregates and bulk soil was significantly positively correlated with the fertilizer-N content in the >2 mm and <0.053 mm fractions, indicating that N retention was coupled with SOC stabilization processes. Compared with RN, RS resulted in a 2−3.4 times greater SOC conversion probability into the <0.053 mm fraction and a 1.4 times higher aggregate-associated fertilizer-N content. SOC fractions differentially regulated the profile distribution of fertilizer-N, with nonlabile organic carbon (C) correlated positively, while dissolved organic C correlated negatively but increased plant N recovery. Compared with RN, RS increased the SOC stock by 24%, reduced NO_3^--N accumulation by 37%, and immobilized 36% more N into the microbial biomass (P<0.05). Our findings demonstrate that straw mulching increases N recovery by mediating SOC fractionation, stabilization, and microbial N immobilization. These results provide new insights into SOC–N interactions that could aid in the development of optimal soil C and N management strategies.

Keywords: fertilizer-nitrogen fate, soil aggregate, soil organic carbon flow, ^{15}N, ^{13}C

1. Introduction

The global agricultural sector heavily relies on intensive nitrogen (N) application to meet the increasing demand for food production (Schulte-Uebbing *et al.* 2022). However, optimizing fertilizer-N efficiency remains a significant challenge, as reactive N is prone to loss through leaching,

Received 31 July 2025; Received in revised form 9 September 2025; Accepted 11 November 2025; Available online 26 December 2025
Cong Xu, E-mail: cxu@jaas.ac.cn; #Correspondence Jidong Wang, E-mail: Jidongwang@jaas.ac.cn

doi: 10.1016/j.jia.2025.12.046

denitrification, and volatilization. These losses not only reduce the efficacy of fertilization but also increase negative environmental impacts (Huddell *et al*. 2020; Singh *et al*. 2025). Consequently, developing strategies to enhance fertilizer-N retention and utilization efficiency is critical for achieving a sustainable balance between agricultural productivity and environmental preservation (Elrys *et al*. 2023).

Straw return has become recognized as a promising practice for managing agricultural waste and improving soil health (Jahangir *et al*. 2021; Lou *et al*. 2023; Yuan *et al*. 2024). Prior studies have shown that the fertilizer-N recovery efficiency under straw return is 9.70%−28.9% greater than that under straw removal (Song F *et al*. 2024; Zhang M *et al*. 2024), highlighting its role in improving fertilizer-N utilization and reducing N losses. These benefits are largely tied to the substantial carbon (C) input from straw return, which results in the significant accumulation of soil organic C (SOC) (Berhane *et al*. 2020; Wang L *et al*. 2023b; Zhao *et al*. 2025). The increase in SOC could benefit the retention of fertilizer-N by promoting soil aggregation (Ramteke and Vashisht 2023; Kelley *et al*. 2024), regulating soil stoichiometry (Xu L *et al*. 2024), and modifying the soil microbial composition (Mondaca *et al*. 2024). Notably, SOC includes different fractions, such as labile and stable components, which play diverse roles in regulating soil N dynamics (Shoumik *et al*. 2025). However, the specific and varied roles of different SOC fractions in regulating the fate of fertilizer-N remain unclear, especially under *in situ* conditions (Yang L *et al*. 2022).

Approximately 90% of the SOC is associated within aggregates (Lugato *et al*. 2021; Wang *et al*. 2025). These aggregates provide physical and chemical stabilization mechanisms that protect SOC from decomposition (Yudina and Kuzyakov 2023). However, owing to pronounced heterogeneity in microenvironments and microbial communities, aggregates of different sizes play distinct roles in regulating SOC fractionation and sequestration (Angst *et al*. 2023; Yudina and Kuzyakov 2023), as evidenced by ^{13}C natural abundance studies showing a primary flow of SOC from macroaggregates to microaggregates for stabilization (Gunina and Kuzyakov 2014; Atere *et al*. 2020; Shi *et al*. 2023). Similarly, the retention of fertilizer-N varies across aggregate fractions: newly applied N is initially immobilized in particulate organic matter within macroaggregates, while subsequent N retention occurs predominantly in silt- and clay-associated organic matter (Zhu *et al*. 2024). These findings suggest that the fate of fertilizer-N is closely linked to SOC transport and transformation patterns at the aggregate scale. Given that straw return has been shown to affect soil aggregation (Poirier *et al*. 2014; Feng *et al*. 2022; Álvaro-Fuentes *et al*. 2025) and the exchange of C between aggregates (Chen P *et al*. 2022), examining SOC flows in conjunction with fertilizer-N dynamics at the aggregate scale could provide deeper insights into how long-term SOC stabilization modulates N retention beyond what bulk soil studies reveal. While linkages between SOC and fertilizer-N can be investigated directly using ^{15}N tracing combined with ^{13}C natural abundance (Wei *et al*. 2023; Wang *et al*. 2025), literature assessing this relationship at the aggregate scale remains scarce.

The Huang-Huai-Hai Plain (HHHP), a typical intensively farmed region with extensive N application in China, serves as both the nation's major cereal production base (Zhang *et al*. 2017; Duan J *et al*. 2021) and a hotspot for N loss (Lei *et al*. 2024). These losses are particularly acute in the southern HHHP because of monsoon rainfall (Ling *et al*. 2021) and elevated temperatures (Shi *et al*. 2013). Given that climate change is expected to increase the frequency of extreme weather events, developing sustainable solutions for such vulnerable areas has become imperative. Since the 1980s, the HHHP has adopted an increasing intensity of straw return, which has led to a 30% increase in SOC content (Liao *et al*. 2015; Berhane *et al*. 2020) and a 13%−61% reduction in fertilizer-N loss (Xu *et al*. 2021; Quan *et al*. 2024). Currently, the incorporation of straw, which is a mixture of straw and soil, is the conventional practice in this region to promote decomposition (Liu *et al*. 2021). In contrast, straw mulching, which involves the application of crop residues to the soil surface, has shown potential to protect soil structure and mitigate soil erosion (Hashimi *et al*. 2020; Parhizkar *et al*. 2021). This surface retention may offer greater advantages in the southern HHHP, where the risk of hydrologically driven N losses is greater. Nonetheless, a critical knowledge gap remains regarding how straw mulching affects the fate of fertilizer-N and its interaction with SOC dynamics (Zhao *et al*. 2025). Consequently, the potential for straw mulching to increase N use efficiency and reduce crop reliance on synthetic fertilizer-N in this region remains unclear.

In this study, a four-year field-based *in situ* ^{15}N-tracing experiment was performed with the following three objectives: i) to elucidate the fate of fertilizer-N at both the soil profile and aggregate scales under different N fertilization and straw management regimes; ii) to investigate the relationships between the fate of fertilizer-N and SOC distribution, fractions and flows; and iii) to assess whether straw mulching can reduce crop reliance on N fertilization. We hypothesized that straw mulching would increase fertilizer-N recovery and that this process would be coupled with SOC stabilization processes. The outcomes of this study would provide insights for optimizing N management in other vulnerable regions worldwide facing similar challenges.

2. Materials and methods

2.1. Study area

The study site is located in Binhai County, Jiangsu Province, China (34°05´48´´N, 119°52´02´´E), which is a typical farming region in the southern HHHP. The site had maintained a winter wheat–summer maize rotation for more than three decades before the experiment began. The region has a temperate monsoonal climate regime, with an average annual temperature of 15.5°C and 964.8 mm of precipitation. The soil is classified as an aquic inceptisol with a sandy loam texture. The top layer (0−20 cm) of soil has a pH of 8.35, a SOC content of 11.03 g kg^{-1}, a total N (TN) content of 1.08 g kg^{-1}, an available phosphorus (P) content of 32.2 mg kg^{-1}, and an available potassium (K) content of 82.3 mg kg^{-1}.

2.2. Experimental design

The field experiment was established in 2018 and included three treatments: conventional N application (FN), reduced N application (RN), and straw return under reduced N application (RS). Each treatment was replicated three times in a completely randomized design, resulting in nine plots (each measuring 4.5 m×7 m). The N application rate was 330 kg N ha^{-1} per season for FN, whereas the RN and RS received 240 kg N ha^{-1} per season. Rotary tillage was performed before wheat sowing, and no tillage was performed before maize sowing across all the treatments. Crop straw was removed after harvest in FN and RN, whereas in RS, the crop straw was chopped into 5−8 cm segments and returned to the soil; the returned straw was incorporated during the wheat season and surface-mulched during the maize season. All treatments were supplied with equivalent amounts of P and K mineral fertilizers at 120 kg P_2O_5 ha^{-1} per season and 90 kg K_2O ha^{-1} per season, respectively. N application consisted of a basal dressing before sowing and topdressing at the jointing stage, applied at a split ratio of 4:6. P and K fertilizers were applied solely as a basal dressing.

In the maize season of 2022, a ^{15}N-labeled microplot was established within each main plot to track the fate of fertilizer-N. Prior to maize sowing, PVC cylinders (25 cm diameter×40 cm length) were inserted to a 30 cm soil depth. The near-background ^{15}N abundance found in soils surrounding the microplots below 30 cm demonstrated that the set cylinder depth provided an effective barrier against lateral N exchange. All N fertilizer applied in the microplots was ^{15}N-labeled (10.05 atom% ^{15}N-urea; Shanghai Chem-Industry Institute, Shanghai, China). The ^{15}N-labeled fertilizer was uniformly applied within the cylinders twice: as basal fertilization and topdressing. Both the fertilization schedule and the application rates of fertilizer and straw in the microplots matched those in the corresponding main plots. Straw from the previous wheat season was surface-mulched in the microplots in the RS treatment. The C and N contents of the applied wheat straw were 27.4% and 0.45%, respectively, and the application rate was 0.90 kg m^{-2}. After the straw application, one maize plant was cultivated per microplot.

2.3. Plant and soil sampling and analyses

At harvest, the aboveground maize grain and straw within each microplot were thoroughly collected, oven-dried at 65°C, weighed, and finely ground for measurement of N content and ^{15}N abundance.

After crop harvest, two replicate soil cores (2.0 cm diameter) were collected from the 0−10, 10−20, 20−40, 40−60, and 60−80 cm soil layers within each microplot. The soil samples were divided into three subsamples: the first subsample was air-dried and ground for analysis of SOC, easily oxidized organic C (EOC), TN, and ^{15}N abundance; the second subsample was stored at 4°C for microbial biomass C (MBC) and microbial biomass N (MBN) analysis; and the third subsample was stored at –20°C for dissolved organic C (DOC), NH_4^+-N, and NO_3^--N analysis. Additional undisturbed soil samples from the 0−10 cm layer were collected using a shovel for aggregate separation.

The aggregates were separated *via* dry- and wet-sieving methods, which were modified from Sey *et al.* (2008) and Shahbaz *et al.* (2016), respectively. Briefly, air-dried soil samples (50 g each) were weighed into stacked sieves with mesh sizes of 2, 0.25, and 0.053 mm. The stacked sieves were then mounted on a shaker and oscillated at 200 cycles min^{-1} for 5 min for dry sieving; wet sieving was performed using a soil aggregate analyzer, where the sieves were automatically oscillated vertically in a water-filled drum at a frequency of 45 times min^{-1} for 5 min. After sieving, the aggregates were classified into four size fractions: >2 mm (large macroaggregate), 0.25–2 mm (small macroaggregate), 0.053−0.25 mm (microaggregates), and <0.053 mm (silt and clay). To avoid potential losses of fertilizer-N and soil C by leaching and dry–wet cycles during wet sieving (Sainju 2006; Blaud *et al.* 2018), dry-sieved samples were used to analyze aggregate-associated TN, SOC, ^{15}N, and ^{13}C. The wet-sieved samples were weighed only to assess the aggregate mass composition and water stability, as the wet-sieving process can cause C and N loss from the aggregates.

The TN contents in the plant and soil samples, along with the SOC content, were analyzed using an elemental analyzer (Vario Macro Cube, Elementar, Germany). For isotopic analysis, the ^{15}N and ^{13}C abundances were measured with an isotope ratio mass spectrometer (Isoprime 100, Elementar, Germany). Before SOC and ^{13}C analysis, the soil samples were pretreated with 1 mol L^{-1} HCl for 12 h to remove carbonates (Shi *et al.* 2017). DOC was extracted with distilled water (1:5, w/v) and quantified using a total organic C analyzer (Multi N/C3100; Analytik Jena, Germany). NH_4^+-N and NO_3^--N were extracted with 1 mol L^{-1} KCl (1:5 w/v) and analyzed *via* a continuous flow analyzer (AA3, SEAL Analytical, Germany). EOC was determined using the 333 mmol L^{-1} $KMnO_4$ oxidation method (Blair *et al.* 1995). Nonlabile organic C (NLOC) was defined as the C that remained unoxidized by $KMnO_4$ and was calculated by subtracting the EOC content from the SOC content. The soil MBC and MBN contents were analyzed *via* the fumigation extraction method (Brookes *et al.* 1985; Vance *et al.* 1987).

To determine soil N runoff losses, an additional microplot (50 cm×50 cm) was established in each plot before maize sowing to measure the runoff volume, and samples were collected after two consecutive precipitation events (June 23rd−July 7th and August 16th−August 24th). The NH_4^+-N, NO_3^--N, and TN contents in the runoff water were analyzed using a continuous flow analyzer (AA3, SEAL Analytical, Germany). Detailed methodologies for runoff collection and soil N runoff loss calculations are provided in Appendix A.

2.4. Calculations

The mean weight diameter (MWD) and geometric mean diameter (GMD) of the soil aggregates (mm) were calculated using the following equations (van Bavel 1950):

$$\text{MWD}=\sum_{i=1}^{n}D_i/\sum_{i=1}^{n}W_i \tag{1}$$

$$\text{GMD}=\text{EXP}\left[\frac{\sum_{i=1}^{n}W_i\ln\overline{x}_i}{\sum_{i=1}^{n}W_i}\right] \tag{2}$$

where D_i is the mean diameter (mm) of the aggregates for each size fraction and W_i is the weight proportion of each size fraction to the total weight of the aggregates.

The magnitude of the contributions (*Contribution*; mg kg^{-1}) of aggregate-associated SOC and TN to the bulk soil was calculated by the following equation:

$$Contribution=Content_{aggregate}\times W_i\times 10^3 \quad (3)$$

where $Content_{aggregate}$ is the aggregate-associated SOC or TN content (g kg^{-1}).

The percentage distributions of SOC and TN in different aggregates were calculated as the ratio of the magnitude of the contribution of aggregate-associated SOC and TN to the SOC (or TN) content of the bulk soil (0−10 cm layer).

The soil stocks (*Stock*) of the soil C and N fractions in each soil layer (Mg ha^{-1} for DOC, EOC, MBC, NLOC, SOC, and TN; kg ha^{-1} for NH_4^+-N, NO_3^--N, and MBN) were calculated by the following equation:

$$Stock=Content\times BD\times H\times 10 \quad (4)$$

where *Content* is the content of soil C and N fractions (g kg^{-1} for DOC, EOC, MBC, NLOC, SOC, and TN; mg kg^{-1} for NH_4^+-N, NO_3^--N, and MBN), *BD* is the soil bulk density (Mg m^{-3}), and *H* is the thickness of the sampled soil layer (m).

The cumulative C or N stocks in the soil profile were calculated by summing the stocks from each soil layer.

The ^{15}N recovery amount (kg N ha^{-1}) within different soil and plant N pools was calculated by the following equations:

$$^{15}\text{N recovery amount}=\%Ndff_{pool}\times N_{mass} \quad (5)$$

$$\%Ndff=(^{15}Nap/^{15}Nap\ fertilizer)\times 100 \quad (6)$$

where $\%Ndff_{pool}$ is the fraction of N derived from fertilizer in the soil and plant N pools (%), N_{mass} (kg N ha^{-1}) is the stock of N within a specific soil N pool or the N uptake in a specific plant part, and ^{15}Nap is the atom% excess of the sample.

The percentage distributions of fertilizer-N at the aggregate, profile, and plant scales were calculated by dividing the amount of fertilizer-N recovered in a specific N pool by the total amount of accumulated fertilizer-N recovered in the aggregates, profiles, or plant parts, respectively. The fertilizer-N recovery efficiency was calculated as the ratio of fertilizer-N recovered in a specific N pool (kg N ha^{-1}) to the total fertilizer-N application rate (kg N ha^{-1}).

The fate of fertilizer-N was categorized into three pathways: crop uptake, soil retention, and the unaccounted portion. Unaccounted fertilizer-N, which was defined as the fertilizer-N lost from the soil profile (Yang *et al.* 2024), was calculated by subtracting the soil- and plant-recovered fertilizer-N from the total fertilizer-N applied. To illustrate C flow among aggregate fractions, a conceptual diagram was developed on the basis of the approaches of Gunina and Kuzyakov (2014) and Chen P *et al.* (2022). δ^{13}C fractionation (Δ^{13}C) values were calculated by subtracting the bulk soil δ^{13}C values from those of specific aggregate fractions. C flows were inferred from the Δ^{13}C gradients, with the arrow origins denoting the presumed source fractions and the arrowheads pointing to the sink fractions (those with higher Δ^{13}C values). Isotopic differentials were quantified as the difference between source and sink compartment Δ^{13}C values, with smaller differences indicating a greater likelihood of C flow between fractions.

2.5. Statistical analysis

Analysis of variance (ANOVA) was performed with SPSS 22.0 software (SPSS Inc., Chicago, IL, USA) to determine the significance of differences (P<0.05) among treatments with the least significant difference (LSD) test. Spearman correlation analysis was conducted to evaluate the relationships between the percentage distributions of SOC and soil N and fertilizer-N in the soil profile using the *corrplot* package in R. The *vegan* and *permute* packages in R were used to conduct redundancy analysis (RDA) for C and N stocks in the soil profile and the overall fate of fertilizer-N and to perform a Monte Carlo permutation test.

Structural equation modeling (SEM) was conducted to identify the direct and indirect factors regulating the percentage distribution of the different fates of fertilizer-N and to evaluate the contributions of straw mulching, the N application rate, and soil parameters. These contributions were quantified by assessing the standardized total effects (the sum of direct and indirect effects). Prior to SEM analysis, the soil parameters were categorized into three groups: 1) soil aggregates (mass composition, MWD, GMD, δ^{13}C, Δ^{13}C, aggregate-associated C, N contents, Ndff%, and fertilizer-N recovery in aggregates); 2) soil C (SOC, EOC, DOC, and MBC) and N stocks (TN, MBN, NH_4^+-N, and NO_3^--N) in the soil profile; and 3) percentage fertilizer-N fates (soil-recovered, plant uptake, and unaccounted). Principal component analysis (PCA) was used to derive multivariate functional indices for each group. The first principal component (PC1) of the soil C and N stocks and fertilizer-N fates, along with the first two components (PC1 and PC2) of the soil aggregate parameters, were retained for subsequent analysis. These selected components explained 56.20%−69.63% of the total variance within their respective groups. PCA was implemented using the *FactoMineR* package in R, while the best-fit SEM was evaluated with AMOS 21.0 (SPSS Inc., Chicago, IL, USA).

3. Results

3.1. Soil aggregate distribution, stability, and associated carbon and nitrogen

Compared with the RN and RS treatments, the FN treatment resulted in significantly greater weight distributions of macroaggregates (0.25−2 mm and >2 mm) under dry sieving, as well as the highest MWD and GMD values across the treatments (Appendix B). Conversely, the proportion of macroaggregate was the lowest in the FN treatment under wet sieving, whereas the macroaggregate distribution, MWD, and GMD were greatest in the RS treatment (P<0.05; Appendix B). More than 68% of the SOC and 60% of the TN were concentrated in the <0.25 mm aggregate fractions (Fig. 1-A and C). Compared with FN, RN reduced the SOC and TN distributions in the 0.25−2 mm fraction but increased them in smaller fractions. Compared with RN, RS resulted in the highest SOC and TN contents in most aggregate fractions (Fig. 1-B and D), with a more uniform distribution of SOC across sizes. However, the TN distributions were comparable between the RN and RS.

3.2. Carbon and nitrogen patterns in soil profiles

SOC and its fractions generally decreased with soil depth across all treatments (Fig. 2-A–D). Compared with FN and

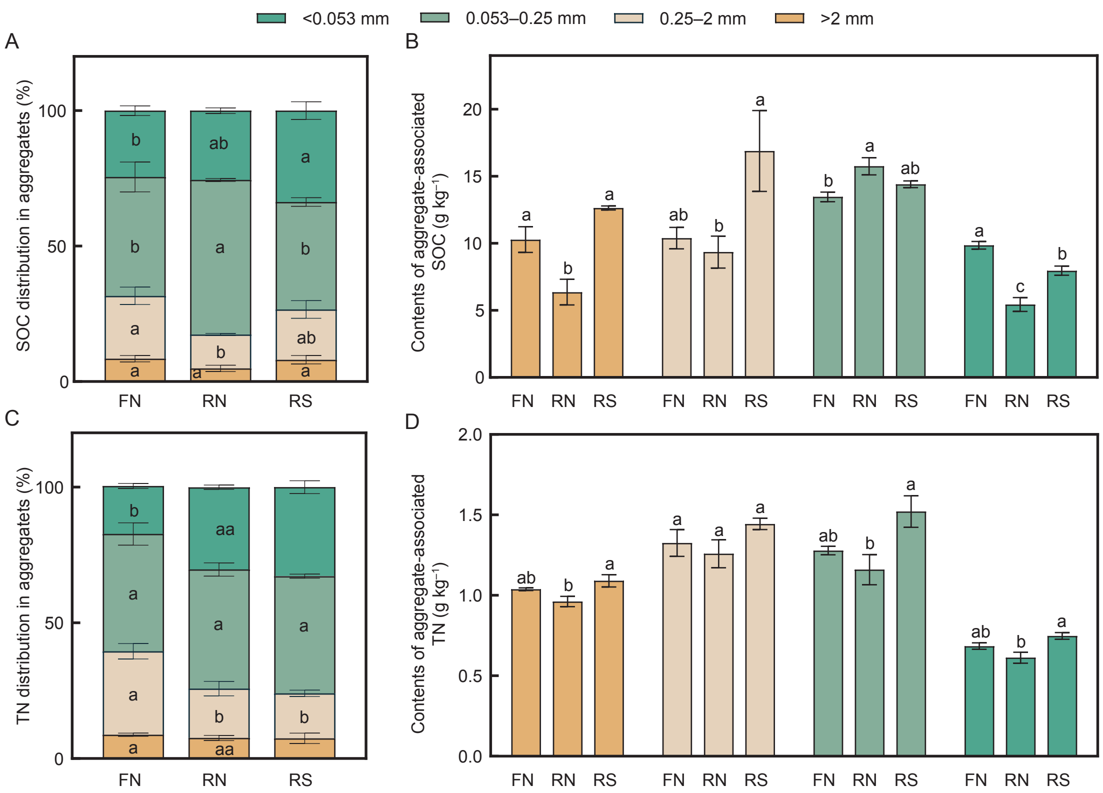

Fig. 1 Soil organic carbon (SOC) (A) and total nitrogen (TN) (C) distributions in soil aggregate fractions, and aggregate-associated SOC (B) and TN (D) contents. FN, conventional N application; RN, reduced N application; RS, reduced N with straw mulching. Different lowercase letters indicate significant differences between treatments at *P*<0.05. Error bars represent the standard error (*n*=3).

RS, RN significantly reduced the SOC and EOC contents throughout the profile, especially at the 0–10 and 40–60 cm depths (*P*<0.05). RN also decreased the DOC, with a significant reduction occurring only at 10–20 cm. In terms of the MBC, compared with the RS and FN, the RN caused notable reductions at 0–10 cm (*P*<0.05). TN, NH_4^+-N, and MBN also decreased with depth (Fig. 2-E, F, and H), whereas NO_3^--N peaked at 40–60 cm (Fig. 2-G). Compared with FN and RN, RS resulted in lower NO_3^--N contents, particularly at 10–20 and 40–60 cm (*P*<0.05), but showed the highest MBN content across 0–60 cm. The patterns of soil C and N distribution were similar to those of their contents (Appendix C). Compared with FN, RN reduced NO_3^--N retention at 0–10 and 60–80 cm. Compared with FN, RS increased the TN and MBN stocks at 0–10 cm but lowered the subsoil NO_3^--N concentration. Compared with that under FN, the SOC stock under RN was significantly lower, while RS resulted in the greatest accumulation (Table 1). NH_4^+-N and NO_3^--N accounted for <2% of the TN. Although the cumulative TN did not differ among the treatments, RS led to significantly higher NH_4^+-N and MBN stocks but lower NO_3^--N stocks than FN and RN.

3.3. Fate of fertilizer-nitrogen in soil aggregates and profiles

At the aggregate scale, RN allocated fertilizer-N predominantly into smaller fractions (0.053–0.25 and <0.053 mm), whereas RS retained more fertilizer-N in macroaggregates (*P*<0.05; Fig. 3-A). The cumulative fertilizer-N recovery amount was greatest for the FN in the aggregates (Fig. 3-B). Compared with RN, RS resulted in greater aggregate-scaled fertilizer-N recovery, driven by significantly greater fertilizer-N retention in the <0.053 mm fraction. Furthermore, the cumulative fertilizer-N recovery efficiency was greatest in the RS, with significant increases concentrated in the 0.25–2 mm and <0.053 mm fractions (Fig. 3-C).

At the profile scale, significant discrepancies in fertilizer-N distribution among the treatments were confined to surface soil layers. Compared with FN and RS, RN allocated a lower proportion of fertilizer-N to the 0–10 cm layer but a higher proportion to the 10–20 cm layer (Fig. 3-D). FN resulted in the highest cumulative fertilizer-N recovery amount, whereas RN and RS resulted in comparable recovery amounts (Fig. 3-E). The fertilizer-N recovery efficiency patterns mostly mirrored those of the recovery distributions and amounts (Fig. 3-F).

Compared with RN and RS, FN distributed a significantly greater proportion of fertilizer-N to crop grains (Fig. 3-G). The fertilizer-N recovery amounts in the crop grains differed markedly among the treatments (*P*<0.05), following the order of FN>RS>RN (Fig. 3-H). RS achieved 35%–36% higher cumulative fertilizer-N recovery efficiency than did FN and RN (*P*<0.05; Fig. 3-I). The overall fertilizer-N fate revealed that 31%–36% of the N was retained in the soil, 22%–31% was utilized by crops, and 38%–46% was unaccounted for. Compared with FN and RN, RS significantly increased soil-retained fertilizer-N and reduced the unaccounted

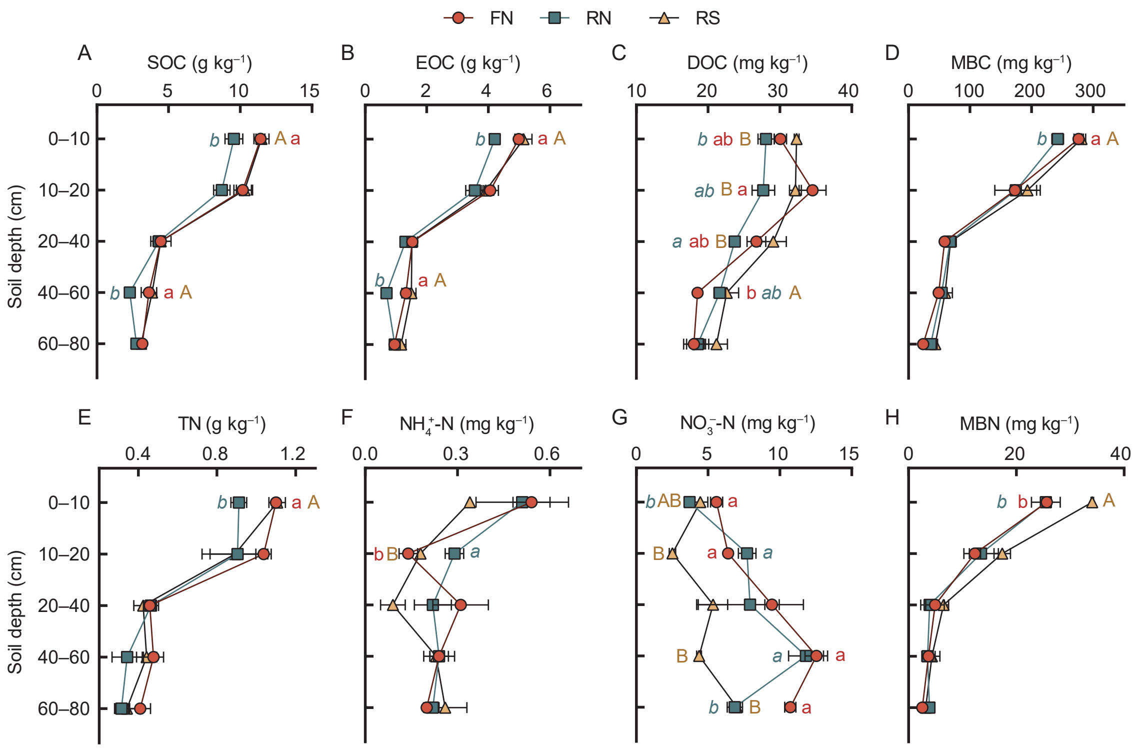

Fig. 2 Contents of soil organic carbon (SOC) (A), easily oxidized organic carbon (EOC) (B), dissolved organic carbon (DOC) (C), microbial biomass carbon (MBC) (D), total nitrogen (TN) (E), NH_4^+-N (F), NO_3^--N (G), and microbial biomass nitrogen (MBN) (H) at different soil depths. FN, conventional nitrogen application; RN, reduced nitrogen application; RS, reduced nitrogen with straw mulching. Regular lowercase, italicized lowercase, and uppercase letters denote the significance labels for FN, RN, and RS treatments, respectively. Different letters indicate significant differences between treatments at $P<0.05$. Error bars represent the standard error (n=3).

Table 1 Cumulative soil carbon and nitrogen stocks within the soil profile[1)]

Treatments[2)]	DOC (Mg ha−1)	EOC (Mg ha−1)	MBC (Mg ha−1)	NLOC (Mg ha−1)	SOC (Mg ha−1)	NH_4^+-N (kg ha−1)	NO_3^--N (kg ha−1)	MBN (kg ha−1)	TN (Mg ha−1)
FN	0.2399 b	20.20 a	0.847 a	33.81 a	54.01 a	0.0712 b	99.01 a	71.12 b	5.96 a
RN	0.2305 b	16.58 b	0.883 a	28.84 a	45.42 b	0.0728 b	82.92 a	72.73 b	5.02 a
RS	0.2686 a	21.93 a	1.0226 a	34.36 a	56.29 a	0.0986 a	51.87 b	98.57 a	5.58 a

[1)] DOC, EOC, MBC, NLOC, SOC, MBN, and TN indicate dissolved organic carbon, easily oxidized organic carbon, microbial biomass carbon, nonlabile organic carbon, soil organic carbon, microbial biomass nitrogen, and total nitrogen, respectively.
[2)] FN, conventional nitrogen application; RN, reduced nitrogen application; RS, reduced nitrogen with straw mulching.
Different letters indicate significant differences among treatments at $P<0.05$.

portion (Fig. 3-J). Additionally, RS significantly decreased unaccounted fertilizer-N by 19%−35% relative to FN and RN (Fig. 3-K).

3.4. Soil organic carbon flows in aggregates

The $\delta^{13}C$ values of aggregate-associated SOC increased with decreasing aggregate size across all the treatments (Appendix D). Compared with FN and RN, RS induced greater $\delta^{13}C$ variations between aggregate fractions and between aggregates and bulk soil, resulting in higher absolute $\Delta^{13}C$ values. The SOC flows indicated predominant transfer pathways from large to small aggregate fractions, either directly or indirectly, in all the treatments (Fig. 4). Relative to the FN, the RN reduced the probability of SOC flows originating from the >2 mm fraction. Compared with the FN, the RS generally exhibited lower probabilities of interaggregate SOC flows. Compared with RN, RS increased the probability of SOC flows originating from the >2 mm fraction but decreased flows between smaller fractions. Correspondingly, the probability of SOC transformation from 0.053−0.25 and 0.25−2 mm to <0.053 mm fractions under RS was 2−3.4 times greater than that under RN.

3.5. Correlations of fertilizer-nitrogen fates with soil parameters

The proportion of macroaggregates (>0.25 mm) was positively related to the SOC stock (0−10 cm) and fertilizer-N recovery efficiency (Appendix E; $P<0.05$). A 1% increase in the macroaggregate proportion corresponded to 0.17 Mg ha−1 higher SOC stock and 0.41% greater fertilizer-N recovery efficiency. The distributions of SOC and fertilizer-N were positively correlated within the aggregates, especially for fractions <2 mm ($P<0.05$; Fig. 5-A–D). Additionally, the $\Delta^{13}C$ was negative in the >2 mm fraction but positive in the

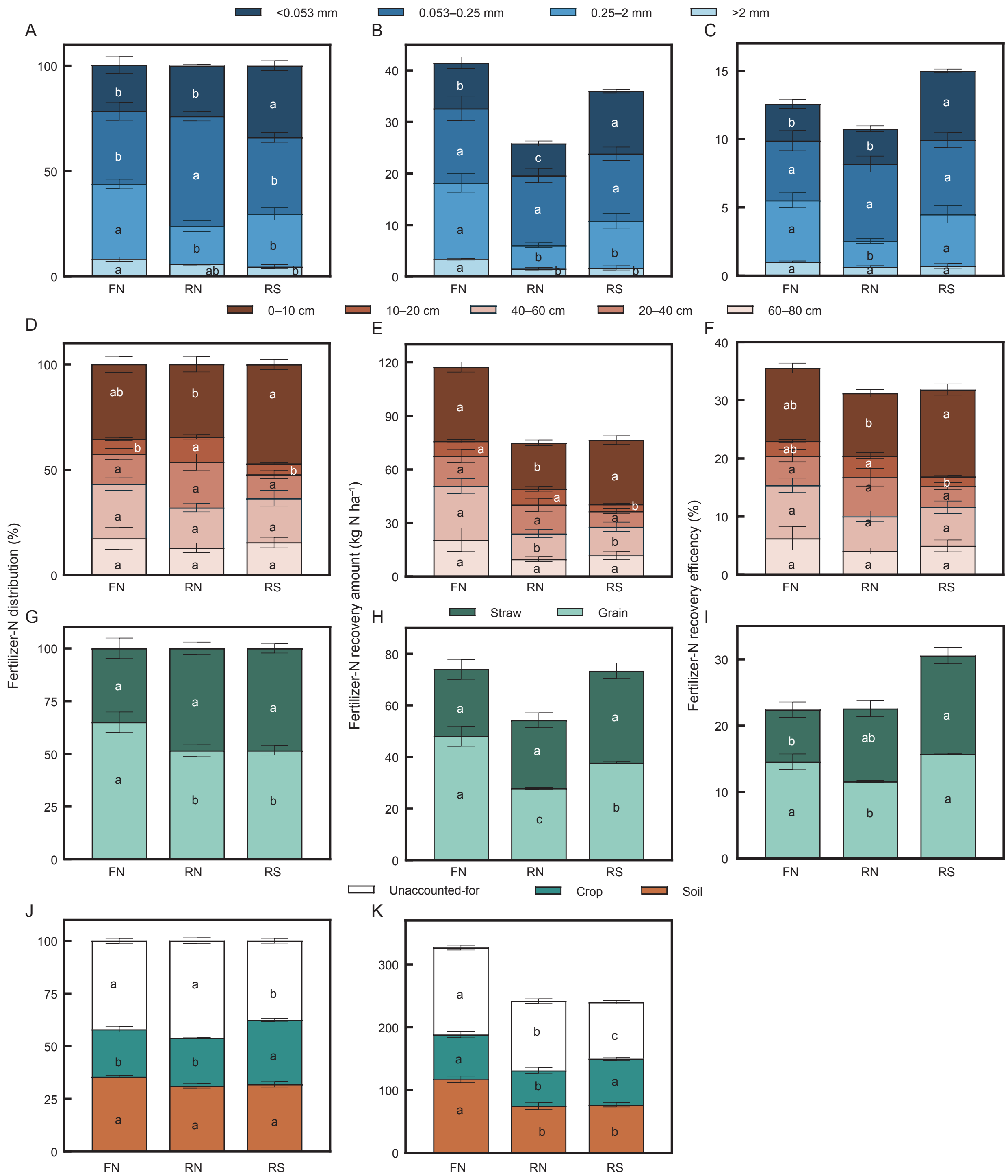

Fig. 3 Fate partitioning of fertilizer-nitrogen (N) across soil aggregate fractions (A, B, and C), soil profiles (D, E, and F), and crop compartments (G, H, and I). The fate of fertilizer-N was quantified through three metrics: percentage distribution (A, D, and G), recovery amount (B, E, and H), and recovery efficiency (C, F, and I). FN, conventional N application; RN, reduced N application; RS, reduced N with straw mulching. The integrated fertilizer-N fates (J and K) summarize the contributions from crop uptake, soil retention, and unaccounted sections, presented as the percentage distribution (J) and cumulative recovery amount (K). Different lowercase letters indicate significant differences between treatments at P<0.05. Error bars represent the standard error (n=3).

<0.053 mm fraction, with both fractions exhibiting positive linear relationships between $\Delta^{13}C$ and aggregate-associated fertilizer-N contents (Fig. 5-E–H).

The fertilizer-N distribution in the soil profile was significantly correlated with the NLOC stock at depths of 20−40 and 40−60 cm, whereas the labile SOC fractions (DOC, EOC, and MBC) had no significant influence (Fig. 6-A–E). The RDA results revealed that the cumulative DOC, EOC, SOC, NLOC, and MBN stocks significantly promoted fertilizer-N recovery in the soil and plants (Fig. 6-F and G). DOC and MBN stocks were most strongly associated with plant fertilizer-N recovery, whereas NO_3^--N stocks tended to

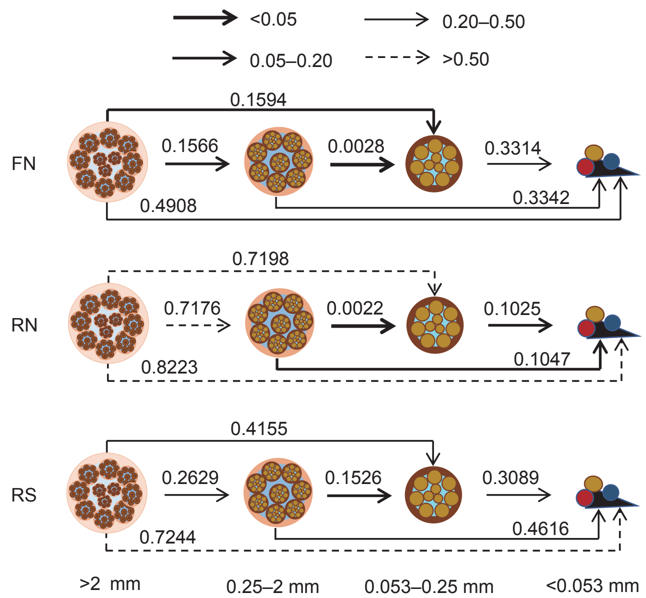

Fig. 4 Pathways of soil organic carbon (SOC) flows between aggregate fractions. The arrows indicate the direction of SOC flow between aggregate fractions. FN, conventional nitrogen application; RN, reduced nitrogen application; RS, reduced nitrogen with straw mulching. The numbers above the arrows represent the probabilities of SOC conversion between the fractions, which were calculated based on the differences in δ^{13}C values between the fractions. The width of the arrows represents the probability of SOC flow; the wider the arrows are, the greater the probability.

increase the amount of unaccounted fertilizer-N.

The SEM indicated that straw mulching and the N application rate either directly affected the fate of fertilizer-N or indirectly influenced it by regulating soil aggregates and soil C and N parameters (Fig. 7). Straw mulching positively affected soil C stocks and the proportion of plant-recovered fertilizer-N but negatively affected the unaccounted portion of fertilizer-N.

4. Discussion

4.1. Nitrogen distributions at the soil aggregate and profile scales

At the aggregate scale, more than half of the soil TN and fertilizer-N were distributed within smaller aggregate sizes (<0.25 mm; Fig. 1). This trend aligns with previous studies conducted by Duan Y *et al.* (2021) and Bhattacharyya *et al.* (2019) but contrasts with that of Chen *et al.* (2025). The observed N distribution pattern in the present study is primarily attributable to the higher mass proportion (>65%; Appendix B) of smaller aggregates (<0.25 mm). In contrast, macroaggregates dominated (>50% soil mass) according to Chen *et al.* (2025). In addition, since macroaggregates facilitate faster N turnover than smaller fractions do (Van Groenigen *et al.* 2002; Duan Y *et al.* 2021), their enhanced mineralization likely promotes N loss or plant uptake, ultimately reducing N distribution proportions.

At the profile scale, fertilizer-N was concentrated mainly in the 0–10 (33%–47%) and 40–60 cm (36%–43%) soil layers (Fig. 3). This finding was inconsistent with previous ^{15}N tracing studies conducted in other regions of the HHHP, which reported that the recovery of fertilizer-N tended to decrease with soil depth (Yang *et al.* 2011; Quan *et al.* 2020).

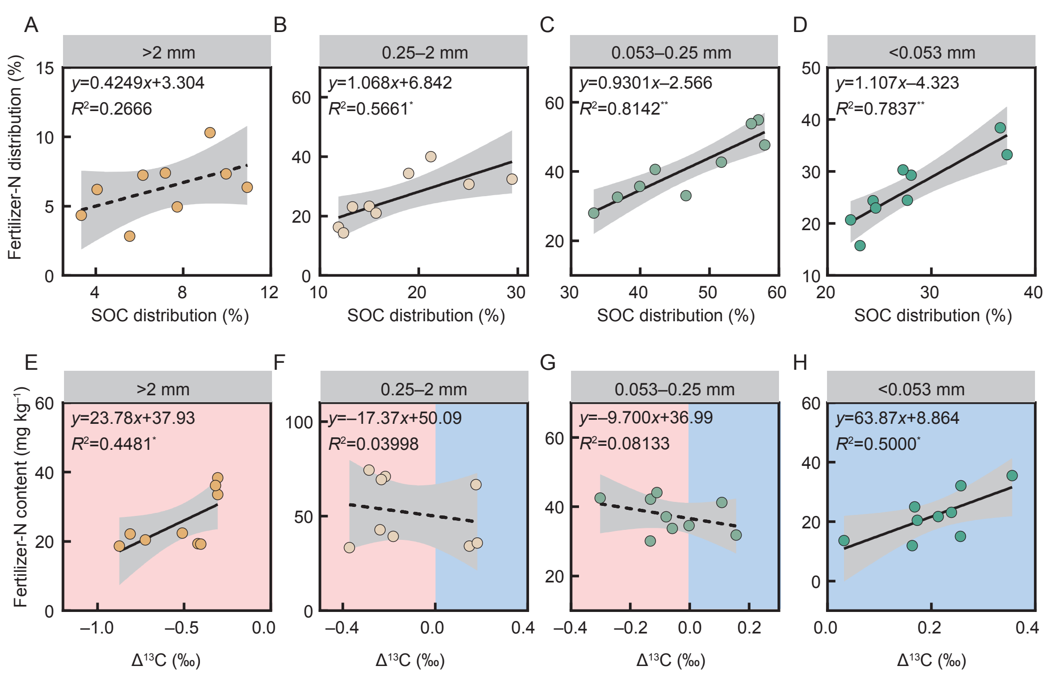

Fig. 5 Linear regressions between the percentage distributions of soil organic carbon (SOC) and fertilizer-nitrogen (N) (A–D), and between Δ^{13}C and the percentage distributions of fertilizer-N (E–H) in different aggregate fractions. Δ^{13}C was determined from the differences in δ^{13}C values between specific aggregate fractions and the bulk soil. Red and blue panels indicate negative and positive Δ^{13}C values, respectively. Solid and dashed lines represent significant and insignificant regressions, respectively. * and ** denote significance at P<0.05 and P<0.01, respectively.

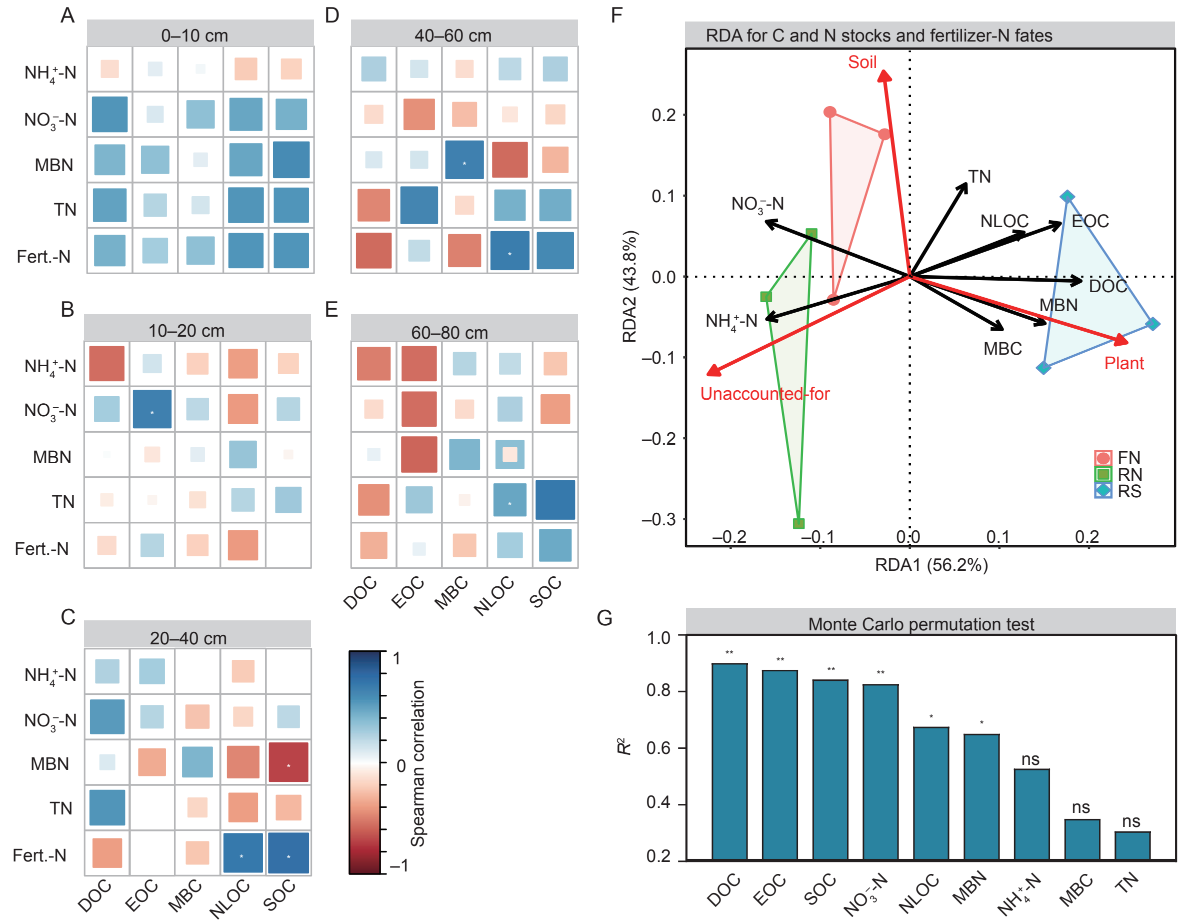

Fig. 6 Spearman correlations between percentage distributions of soil organic carbon and soil nitrogen (N) and fertilizer-N (Fert.-N) at 0–10 (A), 10–20 (B), 20–40 (C), 40–60 (D), and 60–80 (E) cm soil depths; redundancy analysis (RDA) for carbon and N stocks in the soil profile and overall fertilizer-N fate (F); and Monte Carlo permutation test for the RDA (G). Soil organic carbon (SOC) and total N (TN) were divided into the fractions dissolved organic carbon (DOC), easily oxidized organic carbon (EOC), microbial biomass carbon (MBC), non-labile organic carbon (NLOC), microbial biomass N (MBN), NH_4^+-N, and NO_3^--N. Red arrows in panel F indicate the fate of fertilizer-N, which is divided into the percentages allocated to soil retention (soil), allocated to plant uptake (plant), and unaccounted for. * and ** denote significance at *P*<0.05 and *P*<0.01, respectively.

One potential reason for fertilizer-N enrichment in deeper soil layers is the significant leaching induced by continuous precipitation (Appendix B; Li *et al.* 2023). Since the aerobic conditions of fluvo-aquic soil are associated with rapid nitrification rates (Xu *et al.* 2023; Zhang Y B *et al.* 2024), NO_3^--N may easily infiltrate deep layers before plant uptake or microbial immobilization (Frick *et al.* 2022; Huddell *et al.* 2023). This mechanism was supported by the congruent distribution patterns of fertilizer-N and soil NO_3^--N throughout the soil profile (Figs. 2 and 3).

4.2. Relationships between soil organic carbon and the fate of fertilizer-nitrogen

An increase in the SOC stock of 1 Mg ha^{-1} was found to increase the total fertilizer-N recovery efficiency by 0.58 percentage points (equivalent to 1.39–1.91 kg N ha^{-1}; Appendix F; *P*<0.01), which aligns with the trends reported in previous global meta-analyses by Xu C *et al.* (2024) and Quan *et al.* (2021). This linkage indicates that, on the basis of the observed straw-induced SOC sequestration rate of 2.71 Mg ha^{-1} yr^{-1}, a reduction in fertilizer-N input of approximately 20 kg ha^{-1} yr^{-1} could be achieved after five years of straw return without compromising the soil N supply.

However, different SOC fractions were found to mediate the fate of fertilizer-N *via* distinct mechanisms (Devêvre and Horwáth 2001). In the present study, the NLOC distribution generally showed a positive linear correlation with the fertilizer-N distribution in the soil profile (Fig. 6), most significantly at 40–60 cm (*P*<0.05). In contrast, the DOC typically exhibited a negative correlation with the soil fertilizer-N distribution. It has been reported that fertilizer-N can be immobilized within necromass and subsequently stabilized in mineral-associated organic matter (MAOM) (Bramble *et al.* 2023; Shoumik *et al.* 2025). The silt and clay fraction have a high capacity to adsorb necromass, which therefore facilitates MAOM formation (Cotrufo *et al.* 2019; Angst *et al.* 2023). This mechanism is supported by the peak δ^{13}C values in the <0.053 mm fraction (Appendix D), indicating that this fraction is associated with the greatest abundance of microbially stabilized C (Atere *et al.* 2020; Shi *et al.* 2023). Consistently, the <0.053 mm fraction showed the strongest positive response in terms of the SOC distribution

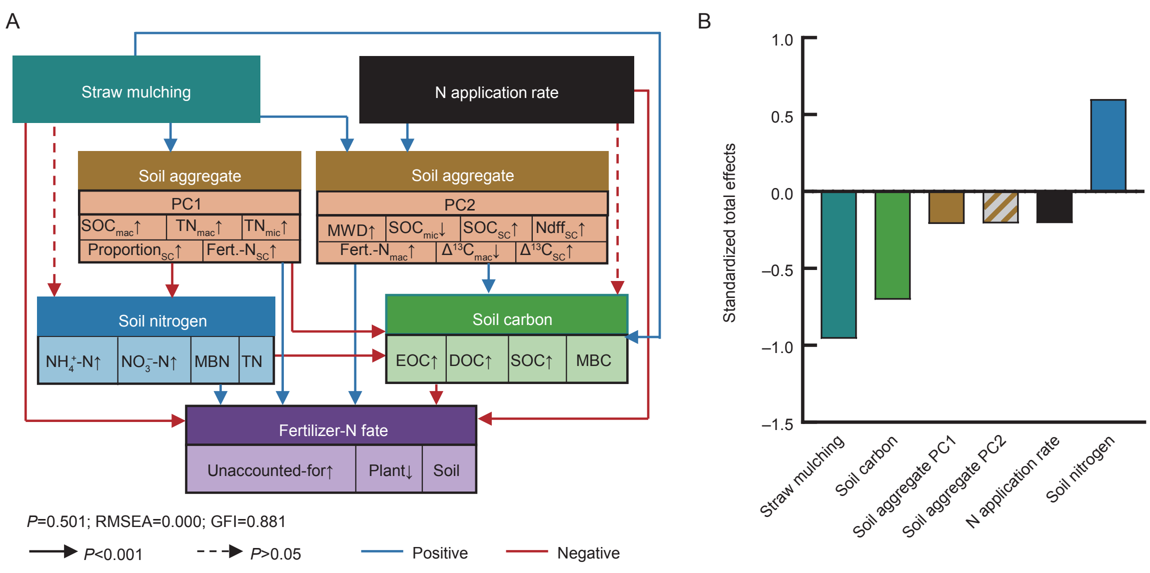

Fig. 7 Structural equation modeling (SEM) results depicting the path model (A) and the standard total effects of straw mulching, nitrogen (N) application rate, and soil parameters (soil aggregate, soil N stock, and soil carbon stock) on the percentage fates of fertilizer-N (B). Arrows indicate the hypothesized direction of causation. Solid and dashed arrows indicate significant and insignificant relationships, respectively. Multiple-layer rectangles represent the first two components from the principal component analysis (PCA) conducted for the soil aggregate-associated parameters and the first component of the PCA for soil N and carbon (C) stocks. SOC_{mac}, TN_{mac}, TN_{mic}, proportion$_{SC}$, and Fert.-N_{SC} in PC1 indicate the macroaggregate-associated soil organic carbon (SOC) content, macroaggregate-associated TN content, microaggregate-associated TN contents, weight proportion of silt and clay, and silt- and clay-associated fertilizer-N content, respectively. MWD, SOC_{mic}, SOC_{SC}, $Ndff_{SC}$, Fert.-N_{mac}, and $\Delta^{13}C_{SC}$ in PC2 represent the mean weight diameter, microaggregate-associated SOC content, silt- and clay-associated SOC content, Ndff% of silt and clay, macroaggregate-associated fertilizer-N content, and absolute $\Delta^{13}C$ value of silt and clay, respectively. Soil C and N parameters included dissolved organic C (DOC), easily oxidized organic C (EOC), microbial biomass C (MBC), nonlabile organic C (NLOC), microbial biomass N (MBN), NH_4^+-N, and NO_3^--N. The arrows "↑" and "↓" indicate significant positive and negative correlations between the variables and the first or second component from the PCA, respectively.

to fertilizer-N and exhibited a robust positive correlation between ^{13}C fractionation and fertilizer-N content (Fig. 5). These results thus suggest that stabilized SOC fractions and their stabilization processes may promote the retention of fertilizer-N in soil.

Notably, the apparent lack of significant, or even negative, correlations between the distributions of DOC and fertilizer-N does not necessarily indicate that higher DOC increases fertilizer-N loss. Instead, the overall crop fertilizer-N recovery efficiency increased significantly with increasing DOC stock (Appendix G). The accumulation of DOC might promote crop yield by increasing the CO_2 supply, soil nutrient availability, and water-holding capacity, which results in high crop uptake of fertilizer-N (He *et al.* 2020; Ren *et al.* 2024). Additionally, crops with greater N recovery from fertilizer generally have greater biomass and produce more root exudates (Morales *et al.* 2023; Li *et al.* 2025), which may in turn release additional DOC to the soil. These findings highlight the importance of considering the diverse roles of SOC fractions in managing fertilizer-N fates and mitigating N losses (Devêvre and Horwáth 2001; Surey *et al.* 2020).

4.3. Reliance of crops on fertilizer-nitrogen and the mitigating effect of straw mulching

Although excessive N fertilizer (>300 kg N ha^{-1}) is conventionally applied in the HHHP to maintain yields (Ju *et al.* 2009), studies have shown that reducing application rates by 24%–60% does not significantly reduce maize yield (Xu *et al.* 2017; Yang Y *et al.* 2022b; Wang L *et al.* 2023a). We adopted a conventional N application rate comparable to that in previous reports (330 kg N ha^{-1}); however, reducing N addition by 27% caused a significant reduction in crop yield (Appendix H). Even with the reduced N application, the N surplus exceeded 110 kg N ha^{-1} in the present study, which theoretically met the crop N requirements (Wang *et al.* 2014; Yin *et al.* 2019). However, the fertilizer-N use efficiency of crops under RN (less than 22%) was significantly lower than that reported under HHHP (mostly over 30%; Fang *et al.* 2006; Ju and Zhang 2017; Chen *et al.* 2023), reflecting a greater reliance of crop productivity on intensive fertilizer-N application than previously assumed.

The precipitation during the experimental period was 542 mm (Appendix I), which already exceeded the mean annual precipitation in northern regions of the HHHP, such as Hebei (460–540 mm; Ling *et al.* 2021). We quantified soil N runoff following two continuous precipitation events. The results revealed that the total N loss *via* runoff was less than 0.8 kg ha^{-1} per event (Appendix J). Considering that 61%–65% of the NO_3^--N stock was sequestered within the deeper soil layers at the end of the cropping season (40–80 cm; Appendix C), the main pathway of hydrologically driven N losses might be the downward leaching of NO_3^--N. In addition, the coarse soil texture in this study could have promoted large pore spaces and reduced water retention capacity, which therefore hindered N retention (Castellano *et al.* 2013; Wang *et al.* 2022). These limitations were exacerbated by a significant SOC deficit. Under RN, compared with the HHHP average of 28 Mg ha^{-1}, the SOC stock in the 0−20 cm layer averaged only 21.0 Mg ha^{-1}, a 25% reduction (Li *et al.* 2024). Furthermore, the mechanical and water stabilities of soil aggregates (MWD<0.40 mm; GMD<0.15 mm; Appendix B) are markedly lower than those in typical literature ranges (0.63−1.73 and 0.59−3.53 mm for MWD and GMD, respectively; Hu *et al.* 2020; Li *et al.* 2020; Wang Y *et al.* 2023), which likely accelerated SOC mineralization and compromised the physical protection of N.

In spite of reduced N application compared with the FN treatment, the RS treatment significantly increased the total fertilizer-N recovery efficiency and comparable crop yield, and markedly reduced the fertilizer-N loss (Fig. 3-I–K), which validates our hypothesis that straw mulching can effectively alleviate the reliance of crops on fertilizer-N. Compared with the RN, the RS resulted in significantly greater amounts of fertilizer-N recovery and efficiency in the 0−10 cm soil layer (Fig. 3-E and F), which was consistent with the findings of a recent ^{15}N-tracing study (Song F *et al.* 2024). The surface application of wheat straw with a high C/N (61 in this study) could allow the microbial utilization of fertilizer-N in the upper soil layer to satisfy the stoichiometric demand for straw decomposition (Yao *et al.* 2017; Wang *et al.* 2021; Chen Z X *et al.* 2022). This was supported by the significantly higher MBN and lower NO_3^--N stocks under RS than under RN (Table 1). Zhou *et al.* (2023) reported that the immobilized fertilizer-N under straw mulching would subsequently be transformed into necromass-N for stabilization. Similarly, the results of the present study revealed that the RS-induced increase in fertilizer-N recovery in the surface soil layer resulted mainly from the increase in aggregate-associated fertilizer-N in <0.053 mm aggregates (96% increase; Fig. 3; P<0.05).

Compared with RN, RS increased the SOC, DOC, and EOC stocks by 24%, 27%, and 32%, respectively (P<0.05; Table 1), which is consistent with previous reports (Yang Y *et al.* 2022a; Song Q *et al.* 2024). Although the NLOC stock did not differ significantly between RN and RS, more than half of the increase in SOC under RS was attributable to elevated NLOC (Table 1). This pattern suggests that straw mulching promotes stable SOC accumulation without significantly increasing native soil C loss through priming effects (Wu *et al.* 2019; Cai *et al*. 2024). Furthermore, compared with that under RN, the water stability of the aggregates under RS was significantly greater (Appendix B), which could strengthen the physical protection of SOC and fertilizer-N, especially during intense rainy seasons (Lin *et al*. 2025). The increased aggregate stability likely resulted from straw-C acting as a core for soil aggregation (Yılmaz *et al.* 2019; Yudina and Kuzyakov 2023), combined with enhanced microbial diversity and enzyme activity promoting fungal hyphal production (Ramteke and Vashisht 2023). In addition to the increase in SOC accumulation, δ^{13}C analysis revealed that the Δ^{13}C values for all aggregate size fractions under RS were greater than those under RN (Appendix D), which was in agreement with the trend observed in a previous study (Chen P *et al.* 2022). These findings indicate that straw mulching promotes the microbial transformation of SOC between aggregate fractions. Considering the significant synergy between SOC transformation and fertilizer-N retention (Fig. 6; Wang *et al.* 2020), the enhanced transformation of SOC under straw mulching might also be conducive to fertilizer-N retention.

4.4. Limitations and implications for future research

Our study offers insights into fertilizer-N dynamics and their potential driving factors at the aggregate and profile scales; however, some limitations remain to be addressed in future research. First, the analysis of the aggregate parameters was confined to the surface soil layer. While the findings emphasize the critical role of upper soil layers in enhancing N retention, evaluating the interactions between aggregate-associated C and fertilizer-N in subsoils could better elucidate N immobilization processes. In addition, although quantifying diverse soil N forms and assessing SOC flows *via* ^{13}C analysis can partially represent soil N and C dynamics, this study lacked specific parameters such as gross N transformation rates and ^{15}N recovery in MAOM. Thus, direct evidence for how fertilizer-N was recovered in specific SOC fractions could not be provided.

Additionally, the observed reductions in fertilizer-N recovery in soil may stem not only from decreased soil retention but also from enhanced plant utilization, indicating that shifts in the fate of fertilizer-N could be mediated by plant N uptake dynamics. Future studies should therefore prioritize investigating the effects of soil–plant interactions on the fate of fertilizer-N and, in particular, how crop straw, root activity, and microbial dynamics govern fertilizer-N transformation and mobility. Given that the results of the present study revealed that fertilizer-N recovery is closely associated with SOC fractionation, stabilization, and microbial N immobilization in straw-mulched soils, future studies should also focus on how combining straw mulching with other organic amendments (Yin *et al.* 2024), soil conditioners (Albalasmeh *et al.* 2021), or microbial inoculants (Ji *et al.* 2024) may further regulate soil aggregation and microbial utilization of N, thereby enhancing N retention under intensive farming.

5. Conclusion

This study revealed a significant reduction in crop yield under reduced N application rates, highlighting the strong reliance of crops on N application. Fertilizer-N retention in soil was closely linked to SOC stabilization processes within aggregates of various sizes. Different SOC fractions played different roles in regulating the fate of fertilizer-N in the soil profile, with NLOC associated with soil N retention and DOC correlated with increased crop N utilization. Overall, straw mulching promoted microbial immobilization of N and strengthened SOC stabilization mechanisms, thereby enhancing fertilizer-N recovery and facilitating a balance between agricultural productivity and reduced reliance on synthetic N in these intensively managed cropland soils.

Acknowledgements

We acknowledge the anonymous reviewers for their helpful comments that significantly improved the manuscript. This work was supported by grants from the National Key R&D

Program of China (2023YFD1901102-04), the National Natural Science Foundation of China (42477314, 42377338, and 42577335), the Basic Research Program of Jiangsu, China (BK20230076), the Jiangsu Agriculture Science and Technology Innovation Fund, China (CX(23)1019), the Key Research and Development Project of Jiangsu Province, China (BE2021378), and the China Agriculture Research System (CARS-10-Sweetpotato).

Declaration of competing interest

The authors declare that they have no conflict of interest.

Declaration of generative AI and AI-assisted technologies in the writing process

The authors declare that they did not use AI in the preparation and writing of this manuscript.

Appendices associated with this paper are available at https://doi.org/10.1016/j.jia.2025.12.046

References

Albalasmeh A A, Hamdan E H, Gharaibeh M A, Hanandeh A E. 2021. Improving aggregate stability and hydraulic properties of Sandy loam soil by applying polyacrylamide polymer. *Soil and Tillage Research*, **206**, 104821.

Álvaro-Fuentes J, Cantero-Martínez C, Alonso-Ayuso M, Gómez F, Ramos M C. 2025. Soil carbon, aggregation and crop residue dynamics under different tillage and nitrogen fertilization strategies in rainfed Mediterranean conditions. *Soil and Tillage Research*, **253**, 106650.

Angst G, Mueller K E, Castellano M J, Vogel C, Wiesmeier M, Mueller C W. 2023. Unlocking complex soil systems as carbon sinks: Multi-pool management as the key. *Nature Communications*, **14**, 2967.

Atere C T, Gunina A, Zhu Z, Xiao M, Liu S, Kuzyakov Y, Chen L, Deng Y, Wu J, Ge T. 2020. Organic matter stabilization in aggregates and density fractions in paddy soil depending on long-term fertilization: Tracing of pathways by ^{13}C natural abundance. *Soil Biology and Biochemistry*, **149**, 107931.

van Bavel C H M. 1950. Mean weight-diameter of soil aggregates as a statistical index of aggregation. *Soil Science Society of America Journal*, **14**, 20–23.

Berhane M, Xu M, Liang Z, Shi J, Wei G, Tian X. 2020. Effects of long-term straw return on soil organic carbon storage and sequestration rate in North China upland crops: A meta-analysis. *Global Change Biology*, **26**, 2686–2701.

Bhattacharyya R, Das T K, Das S, Dey A, Patra A K, Agnihotri R, Ghosh A, Sharma A R. 2019. Four years of conservation agriculture affects topsoil aggregate-associated ^{15}nitrogen but not the ^{15}nitrogen use efficiency by wheat in a semi-arid climate. *Geoderma*, **337**, 333–340.

Blair G, Lefroy R, Lisle L. 1995. Soil carbon fractions based on their degree of oxidation, and the development of a carbon management index for agricultural systems. *Australian Journal of Agricultural Research*, **46**, 393–406.

Blaud A, van der Zaan B, Menon M, Lair G J, Zhang D, Huber P, Schiefer J, Blum W E H, Kitzler B, Wei E H, van Gaans P, Banwart S. 2018. The abundance of nitrogen cycle genes and potential greenhouse gas fluxes depends on land use type and little on soil aggregate size. *Applied Soil Ecology*, **125**, 1–11.

Bramble S E, Ulrich S, Schoning I, Mikutta R, Brandt L, Poll C, Kandeler E, Mikutta C, Konrad A, Siemens J, Yang Y, Polle A, Schall P, Ammer C, Kaiser K, Schrumpf M. 2023. Formation of mineral-associated organic matter in temperate soils is primarily controlled by mineral type and modified by land use and management intensity. *Global Change Biology*, **30**, e17024.

Brookes P C, Kragt J F, Powlson D S, Jenkinson D S. 1985. Chloroform fumigation and the release of soil nitrogen: The effects of fumigation time and temperature. *Soil Biology and Biochemistry*, **17**, 831–835.

Cai S, Sun L, Wang W, Li Y, Ding J, Jin L, Li Y, Zhang J, Wang J, Wei D. 2024. Straw mulching alters the composition and loss of dissolved organic matter in farmland surface runoff by inhibiting the fragmentation of soil small macroaggregates. *Journal of Integrative Agriculture*, **23**, 1703–1717.

Castellano M J, Lewis D B, Kaye J P. 2013. Response of soil nitrogen retention to the interactive effects of soil texture, hydrology, and organic matter. *Journal of Geophysical Research* (Biogeosciences), **118**, 280–290.

Chen A, Zhu B, Chen C, Wei Z, Ma G, Qin H, Hou H, Yi Z. 2025. Sensitivity of aggregate-associated soil organic carbon and total nitrogen to abandonment of paddy soil in subtropical China. *Plant and Soil*, **508**, 193–208.

Chen B, Ren C, Wang C, Duan J, Reis S, Gu B. 2023. Driving forces of nitrogen use efficiency in Chinese croplands on county scale. *Environmental Pollution*, **316**, 120610.

Chen P, Xu J, Zhang Z, Wang K, Li T, Wei Q, Li Y. 2022. Carbon pathways in aggregates and density fractions in Mollisols under water and straw management: Evidence from ^{13}C natural abundance. *Soil Biology and Biochemistry*, **169**, 108684.

Chen Z X, Elrys A S, Zhang H M, Tu X S, Wang J, Cheng Y, Zhang J B, Cai Z C. 2022. How does organic amendment affect soil microbial nitrate immobilization rate? *Soil Biology and Biochemistry*, **173**, 108784.

Cotrufo M F, Ranalli M G, Haddix M L, Six J, Lugato E. 2019. Soil carbon storage informed by particulate and mineral-associated organic matter. *Nature Geoscience*, **12**, 989–994.

Devêvre O C, Horwáth W R. 2001. Stabilization of fertilizer nitrogen-15 into humic substances in aerobic vs. waterlogged soil following straw incorporation. *Soil Science Society of America Journal*, **65**, 499–510.

Duan J, Ren C, Wang S, Zhang X, Reis S, Xu J, Gu B. 2021. Consolidation of agricultural land can contribute to agricultural sustainability in China. *Nature Food*, **2**, 1014–1022.

Duan Y, Yang H, Shi T, Zhang W, Xu M, Gao S. 2021. Long-term manure application to improve soil macroaggregates and plant-available nitrogen in a Mollisol. *Soil & Tillage Research*, **211**, 105035.

Elrys A S, Wang J, Meng L, Zhu Q, El-Sawy M M, Chen Z, Tu X, El-Saadony M T, Zhang Y, Zhang J, Cai Z, Muller C, Cheng Y. 2023. Integrative knowledge-based nitrogen management practices can provide positive effects on ecosystem nitrogen retention. *Nature Food*, **4**, 1075–1089.

Fang Q, Yu Q, Wang E, Chen Y, Zhang G, Wang J, Li L. 2006. Soil nitrate accumulation, leaching and crop nitrogen use as influenced by fertilization and irrigation in an intensive wheat–maize double cropping system in the North China Plain. *Plant and Soil*, **284**, 335–350.

Feng X, Xia X, Chen S, Lin Q, Zhang X, Cheng K, Liu X, Bian R, Zheng J, Li L, Joseph S, Drosos M, Pan G. 2022. Amendment of crop residue in different forms shifted micro-pore system structure and potential functionality of macroaggregates while changed their mass proportion and carbon storage of paddy topsoil. *Geoderma*, **409**, 115643.

Frick H, Oberson A, Frossard E, Bünemann E K. 2022. Leached nitrate under fertilised loamy soil originates mainly from mineralisation of soil organic N. *Agriculture, Ecosystems & Environment*, **338**, 108093.

Van Groenigen K J, Harris D, Horwath W R, Hartwig U A, Van Kessel C. 2002. Linking sequestration of ^{13}C and ^{15}N in aggregates in a pasture soil following 8 years of elevated atmospheric CO_2. *Global Change Biology*, **8**, 1094–1108.

Gunina A, Kuzyakov Y. 2014. Pathways of litter C by formation of aggregates and SOM density fractions: Implications from ^{13}C natural abundance. *Soil Biology and Biochemistry*, **71**, 95–104.

Hashimi R, Kaneda S, Kaneko N, Ohta H, Komatsuzaki M. 2020. Aggregate distribution and substrate-induced respiration under different tillage and mulching management systems in organic farming. *Soil Science and Plant Nutrition*, **66**, 878–888.

He Y, Cheng W, Zhou L, Shao J, Liu H, Zhou H, Zhu K, Zhou X. 2020. Soil DOC release and aggregate disruption mediate rhizosphere priming effect on soil C decomposition. *Soil Biology and Biochemistry*, **144**, 107787.

Hu X, Chen J, Zhu L. 2020. Soil aggregate size distribution and stability of farmland as affected by dry and wet sieving methods. *Zemdirbyste-Agriculture*, **107**, 179–184.

Huddell A, Ernfors M, Crews T, Vico G, Menge D N L. 2023. Nitrate leaching losses and the fate of ^{15}N fertilizer in perennial intermediate wheatgrass and annual wheat — A field study. *Science of the Total Environment*, **857**, 159255.
Huddell A M, Galford G L, Tully K L, Crowley C, Palm C A, Neill C, Hickman J E, Menge D N L. 2020. Meta-analysis on the potential for increasing nitrogen losses from intensifying tropical agriculture. *Global Change Biology*, **26**, 1668–1680.
Jahangir M M R, Begum R, Jahiruddin M, Dawar K, Zaman M, Bell R W, Richards K G, Müller C. 2021. Reduced tillage with residue retention and nitrogen application rate increase N_2O fluxes from irrigated wheat in a subtropical floodplain soil. *Agriculture*, *Ecosystems & Environment*, **306**, 107194.
Ji C, Wang J, Sun Y, Xu C, Zhou J, Zhong Y, Ning Y, Zhang H, Zhang Y, Chen Y. 2024. Wheat straw and microbial inoculants have an additive effect on N_2O emissions by changing microbial functional groups. *European Journal of Soil Science*, **75**, e13494.
Ju X T, Xing G X, Chen X P, Zhang S L, Zhang L J, Liu X J, Cui Z L, Yin B, Christie P, Zhu Z L, Zhang F S. 2009. Reducing environmental risk by improving N management in intensive Chinese agricultural systems. *PLoS ONE*, **106**, 3041–3046.
Ju X T, Zhang C. 2017. Nitrogen cycling and environmental impacts in upland agricultural soils in North China: A review. *Journal of Integrative Agriculture*, **16**, 2848–2862.
Kelley L A, Zhang Z, Tamagno S, Lundy M E, Mitchell J P, Gaudin A C M, Pittelkow C M. 2024. Changes in soil N_2O emissions and nitrogen use efficiency following long-term soil carbon storage: Evidence from a mesocosm experiment. *Agriculture*, *Ecosystems & Environment*, **370**, 109054.
Lei S, Zhao M, Zhu H, Xia M, Chen Z, Zhou J. 2024. Fates and controlling factors of nitrogen fertilizers in relation to grain yield after the application season in wheat cropping systems: A meta-analysis of ^{15}N field trials. *Field Crops Research*, **310**, 109364.
Li D X, Zhang T T, Yu H H, Li Y, Lv T, Yu D, Liu C H. 2025. The impacts of different nitrogen supply on root traits, root exudates, and soil enzyme activities of exotic and native plant communities. *Plant and Soil*, **508**, 209–226.
Li T, Zhang Y, Bei S, Li X, Reinsch S, Zhang H, Zhang J. 2020. Contrasting impacts of manure and inorganic fertilizer applications for nine years on soil organic carbon and its labile fractions in bulk soil and soil aggregates. *Catena*, **194**, 104739.
Li W, Ma L, Shi F, Wang S, Zhao J, Zheng W, Li Z, Li Z, Zhai B. 2023. Regulation of soil water and nitrate by optimizing nitrogen fertilization and the addition of manure based on precipitation: An 8-year field record. *Agriculture*, *Ecosystems & Environment*, **354**, 108586.
Li Y, Ma P, Wu Z, Chen J, Zhao Y. 2024. Estimating spatiotemporal variations of cropland soil organic carbon and its sequestration potential in central China from 1984 to 2019. *Catena*, **245**, 108333.
Liao Y, Wu W L, Meng F Q, Smith P, Lal R. 2015. Increase in soil organic carbon by agricultural intensification in northern China. *Biogeosciences*, **12**, 1403–1413.
Lin H, Zheng J, Zhou M, Xu P, Lan T, Kuang F, Li Z, Yao Z, Zhu B. 2025. Crop straw incorporation increases the soil carbon stock by improving the soil aggregate structure without stimulating soil heterotrophic respiration. *Journal of Integrative Agriculture*, **24**, 1542–1561.
Ling M, Han H, Wei X, Lv C. 2021. Temporal and spatial distributions of precipitation on the Huang-Huai-Hai Plain during 1960–2019, China. *Journal of Water and Climate Change*, **12**, 2232–2244.
Liu N, Li Y, Cong P, Wang J, Guo W, Pang H, Zhang L. 2021. Depth of straw incorporation significantly alters crop yield, soil organic carbon and total nitrogen in the North China Plain. *Soil & Tillage Research*, **205**, 104772.
Lou C, Zhang Y, McLaughlin N B, Gao Y, Zhou R, Zhang Y, Liu H, Huang D, Chen X, Zhang S, Chen W, Liang A. 2023. Changes in soil total nitrogen induced by crop residue return: A meta-analysis. *Soil & Tillage Research*, **230**, 105712.
Lugato E, Lavallee J M, Haddix M L, Panagos P, Cotrufo M F. 2021. Different climate sensitivity of particulate and mineral-associated soil organic matter. *Nature Geoscience*, **14**, 295–300.
Mondaca P, Celis-Diez J L, Díaz-Siefer P, Olmos-Moya N, Montero-Silva F, Molina S, Fontúrbel F E, Aponte H, Mandakovic D, Bastidas B, Arellano E C, Lavandero B, Carvajal M, Gaxiola A. 2024. Effects of sustainable agricultural practices on soil microbial diversity, composition, and functions. *Agriculture*, *Ecosystems & Environment*, **370**, 109053.
Morales M E, Iocoli G A, Allegrini M, Villamil M B, Zabaloy M C. 2023. Response of root exudates and bacterial community to N fertilization and termination methods in *Avena sativa* L. as a winter cover crop model. *European Journal of Soil Biology*, **114**, 103453.
Parhizkar M, Shabanpour M, Lucas-Borja M E, Zema D A, Li S, Tanaka N, Cerdà A. 2021. Effects of length and application rate of rice straw mulch on surface runoff and soil loss under laboratory simulated rainfall. *International Journal of Sediment Research*, **36**, 468–478.
Poirier V, Angers D A, Whalen J K. 2014. Formation of millimetric-scale aggregates and associated retention of ^{13}C–^{15}N-labelled residues are greater in subsoil than topsoil. *Soil Biology and Biochemistry*, **75**, 45–53.
Quan Z, Li S, Xun Z, Liu C, Liu D, Wang Y, Zhao X, Yang M, Lu C, Chen X, Fang Y. 2024. Evaluating the effects of reduced n application, a nitrification inhibitor, and straw incorporation on fertilizer-N fates in the maize growing season: A field ^{15}N tracer study. *Nitrogen*, **5**, 584–597.
Quan Z, Li S, Zhang X, Zhu F, Li P, Sheng R, Chen X, Zhang L M, He J Z, Wei W, Fang Y. 2020. Fertilizer nitrogen use efficiency and fates in maize cropping systems across China: Field ^{15}N tracer studies. *Soil & Tillage Research*, **197**, 104498.
Quan Z, Zhang X, Davidson E A, Zhu F, Li S, Zhao X, Chen X, Zhang L M, He J Z, Wei W, Fang Y. 2021. Fates and use efficiency of nitrogen fertilizer in maize cropping systems and their responses to technologies and management practices: A global analysis on field ^{15}N tracer studies. *Earth's Future*, **9**, e2020EF001514.
Ramteke P, Vashisht B B. 2023. Soil aggregates associated carbon and enzyme activities under long-term nitrogen and rice straw incorporation in Rice-Wheat system. *Communications in Soil Science and Plant Analysis*, **54**, 2519–2534.
Ren T, Ukalska-Jaruga A, Smreczak B, Cai A. 2024. Dissolved organic carbon in cropland soils: A global meta-analysis of management effects. *Agriculture*, *Ecosystems & Environment*, **371**, 109080.
Sainju U M. 2006. Carbon and nitrogen pools in soil aggregates separated by dry and wet sieving methods. *Soil Science*, **171**, 937–949.
Schulte-Uebbing L F, Beusen A H W, Bouwman A F, de Vries W. 2022. From planetary to regional boundaries for agricultural nitrogen pollution. *Nature*, **610**, 507–512.
Sey B K, Manceur A M, Whalen J K, Gregorich E G, Rochette P. 2008. Small-scale heterogeneity in carbon dioxide, nitrous oxide and methane production from aggregates of a cultivated sandy-loam soil. *Soil Biology and Biochemistry*, **40**, 2468–2473.
Shahbaz M, Kuzyakov Y, Heitkamp F. 2016. Decrease of soil organic matter stabilization with increasing inputs: Mechanisms and controls. *Geoderma*, **304**, 76–82.
Shi H J, Wang X J, Zhao Y J, Xu M G, Li D W, Guo Y. 2017. Relationship between soil inorganic carbon and organic carbon in the wheat–maize cropland of the North China Plain. *Plant and Soil*, **418**, 423–436.
Shi J, Deng L, Gunina A, Alharbi S, Wang K, Li J, Liu Y, Shangguan Z, Kuzyakov Y. 2023. Carbon stabilization pathways in soil aggregates during long-term forest succession: Implications from $\delta^{13}C$ signatures. *Soil Biology and Biochemistry*, **180**, 108988.
Shi W, Tao F, Liu J. 2013. Regional temperature change over the Huang-Huai-Hai Plain of China: The roles of irrigation versus urbanization. *International Journal of Climatology*, **34**, 1181–1195.
Shoumik B A A, Khan M Z, Błońska E, Lasota J. 2025. Dynamics of soil organic carbon and total nitrogen in particulate and mineral-associated organic matter fractions under different continuous land use patterns across Europe. *Agriculture*, *Ecosystems & Environment*, **381**, 109411.
Singh A, Rudnick D, Snow D, Misar C, Birru G, Proctor C, Puntel L, Iqbal J. 2025. Intra-and inter-annual variability of nitrogen and irrigation management effects on nitrate leaching and maize yield in the Bazile Groundwater Management Area, Nebraska. *Agriculture*, *Ecosystems & Environment*, **381**, 109463.
Song F, Liu M, Zhang Z, Qi Z, Li T, Du S, Li A, Liu J. 2024. No-tillage with straw mulching increased maize yield and nitrogen fertilizer recovery rate in northeast China. *Agricultural Water Management*, **292**, 108687.
Song Q, Yang B, Xu M, Zhang F, Liu Q, Li S. 2024. A three-year record of CO_2, CH_4 and N_2O emissions in maize fields influenced by mulching methods on the Loess Plateau, China. *Agriculture*, *Ecosystems & Environment*, **367**, 108963.
Surey R, Lippold E, Heilek S, Sauheitl L, Henjes S, Horn M A, Mueller

C W, Merbach I, Kaiser K, Böttcher J, Mikutta R. 2020. Differences in labile soil organic matter explain potential denitrification and denitrifying communities in a long-term fertilization experiment. *Applied Soil Ecology*, **153**, 103630.
Vance E D, Brookes P C, Jenkinson D S. 1987. An extraction method for measuring soil microbial biomass C. *Soil Biology and Biochemistry*, **19**, 703–707.
Wang G L, Chen X P, Cui Z L, Yue S C, Zhang F S. 2014. Estimated reactive nitrogen losses for intensive maize production in China. *Agriculture Ecosystems & Environment*, **197**, 293–300.
Wang J, Chen Z, Xu C, Elrys A S, Shen F, Cheng Y, Chang S X. 2021. Organic amendment enhanced microbial nitrate immobilization with negligible denitrification nitrogen loss in an upland soil. *Environmental Pollution*, **288**, 117721.
Wang L, He D, Wang E, Chen G, Li Z, Qian X, Gao Y, Zhang H, Liu K. 2023a. Nitrogen management to reduce GHG emissions while maintaining high crop productivity in temperate summer rainfall climate. *Field Crops Research*, **290**, 108761.
Wang L, He Z, Zhao W, Wang C, Ma D. 2022. Fine soil texture is conducive to crop productivity and nitrogen retention in irrigated cropland in a desert-oasis ecotone, northwest China. *Agronomy*, **12**, 1509.
Wang L, Wang E, Qian X, Gao Y, Zhang H, Li Z, Liu K. 2023b. Optimal straw management co-benefits crop yield and soil carbon sequestration of intensive farming systems. *Land Degradation & Development*, **34**, 2322–2333.
Wang X, Wang C, Cotrufo M F, Sun L, Jiang P, Liu Z, Bai E. 2020. Elevated temperature increases the accumulation of microbial necromass nitrogen in soil via increasing microbial turnover. *Global Change Biology*, **26**, 5277–5289.
Wang Y, Gunina A, Yang D, Sun T, Kuzyakov Y. 2025. Carbon pathways in soil: Unraveled by ^{13}C natural abundance. *Soil Biology and Biochemistry*, **209**, 109872.
Wang Y, Wu P, Qiao Y, Li Y, Liu S, Gao C, Liu C, Shao J, Yu H, Zhao Z, Guan X, Wen P, Wang T. 2023. The potential for soil C sequestration and N fixation under different planting patterns depends on the carbon and nitrogen content and stability of soil aggregates. *Science of the Total Environment*, **897**, 165430.
Wei J, Knicker H, Zhou Z, Eckhardt K U, Leinweber P, Wissel H, Yuan W, Brüggemann N. 2023. Nitrogen immobilization caused by chemical formation of black-and amide-N in soil. *Geoderma*, **429**, 116274.
Wu L, Zhang W, Wei W, He Z, Kuzyakov Y, Bol R, Hu R. 2019. Soil organic matter priming and carbon balance after straw addition is regulated by long-term fertilization. *Soil Biology and Biochemistry*, **135**, 383–391.
Xu C, Han X, Bol R, Smith P, Wu W, Meng F. 2017. Impacts of natural factors and farming practices on greenhouse gas emissions in the North China Plain: A meta-analysis. *Ecology and Evolution*, **7**, 6702–6715.
Xu C, Han X, Zhuge Y, Xiao G, Ni B, Xu X, Meng F. 2021. Crop straw incorporation alleviates overall fertilizer-N losses and mitigates N_2O emissions per unit applied N from intensively farmed soils: An *in situ* ^{15}N tracing study. *Science of the Total Environment*, **764**, 142884.
Xu C, Zhu H, Liu H, Ji C, Yuan J, Li G, Wang J, Zhang Y. 2024. Patterns of crop-specific fertilizer-nitrogen losses and opportunities for sustainable mitigation: A quantitative overview of ^{15}N-tracing studies. *Soil Ecology Letters*, **6**, 230206.
Xu C, Zhu H, Wang J, Ji C, Liu Y, Chen D, Zhang H, Wang J, Zhang Y. 2023. Fertilizer N triggers native soil N-derived N_2O emissions by priming gross N mineralization. *Soil Biology and Biochemistry*, **178**, 108961.
Xu L, Chen H, Zhou Y, Zhang J, Nadeem M Y, Miao C, You J, Li W, Jiang Y, Ding Y, Li G. 2024. Long-term straw returning improved soil nitrogen sequestration by accelerating the accumulation of amino acid nitrogen. *Agriculture, Ecosystems & Environment*, **362**, 108846.
Yang G, Kang J, Wang Y, Zhao X, Wang S. 2024. Environmental transport of excess nitrogen fertilizer in peach orchard: Evidence arising from ^{15}N tracing trial. *Agriculture*, *Ecosystems & Environment*, **370**, 109066.
Yang L, Liu W, Jia Z, Li P, Wu Y, Chen Y, Liu C, Chang P, Liu L. 2022. Land-use change reduces soil nitrogen retention of both particulate and mineral-associated organic matter in a temperate grassland. *Catena*, **216**, 106432.
Yang Y, Bao X, Xie H, He H, Zhang X, Shao P, Zhu X, Jiang Y, Liang C. 2022a. Frequent stover mulching builds healthy soil and sustainable agriculture in Mollisols. *Agriculture*, *Ecosystems & Environment*, **326**, 107815.
Yang Y, Wang X, Dai K, Jia S, Meng C, Zhao Q, Zhang X, Zhang D, Feng Z, Sun Y, Wu X, Cai D, Grant C. 2011. Fate of labeled urea-^{15}N as basal and topdressing applications in an irrigated wheat–maize rotation system in North China plain: II summer maize. *Nutrient Cycling in Agroecosystems*, **90**, 379–389.
Yang Y, Zou J, Huang W, Manevski K, Olesen J E, Rees R M, Hu S, Li W, Kersebaum K C, Louarn G, Ferchaud F, Si J, Xiong S, Wen X, Chen F, Yin X. 2022b. Farm-scale practical strategies to increase nitrogen use efficiency and reduce nitrogen footprint in crop production across the North China Plain. *Field Crops Research*, **283**, 108526.
Yao Z, Yan G, Zheng X, Wang R, Liu C, Butterbach-Bahl K. 2017. Straw return reduces yield-scaled N_2O plus NO emissions from annual winter wheat-based cropping systems in the North China Plain. *Science of the Total Environment*, **590–591**, 174–185.
Yılmaz E, Çanakcı M, Topakcı M, Sönmez S, Ağsaran B, Alagöz Z, Çıtak S, Uras D S. 2019. Effect of vineyard pruning residue application on soil aggregate formation, aggregate stability and carbon content in different aggregate sizes. *Catena*, **183**, 104219.
Yin Y, Chen Z, Gong H, He K, Miao Q, Tian X, Wang Z, Wang Y, Zheng H, Cui Z. 2024. Soil organic carbon formation efficiency from straw/stover and manure input and its drivers: Estimates from long-term data in global croplands. *Global Change Biology*, **30**, e17460.
Yin Y, Ying H, Xue Y, Zheng H, Zhang Q, Cui Z. 2019. Calculating socially optimal nitrogen (N) fertilization rates for sustainable N management in China. *Science of the Total Environment*, **688**, 1162–1171.
Yuan S, Li R, Zhang Y, Luan H, Tang J, Wang L, Ji H, Huang S. 2024. Effects of long-term partial substitution of inorganic fertilizer with pig manure and/or straw on nitrogen fractions and microbiological properties in greenhouse vegetable soils. *Journal of Integrative Agriculture*, **23**, 2083–2098.
Yudina A, Kuzyakov Y. 2023. Dual nature of soil structure: The unity of aggregates and pores. *Geoderma*, **434**, 116478.
Zhang M, Yang N, Wang S, Han X, Dang P, Li G, Wen S, Zhang L, Xue J, Qin X, Siddique K H M. 2024. Straw returning and nitrogen reduction: Strategies for sustainable maize production in the dryland. *Journal of Environmental Management*, **366**, 121837.
Zhang X, Bol R, Rahn C, Xiao G, Meng F, Wu W. 2017. Agricultural sustainable intensification improved nitrogen use efficiency and maintained high crop yield during 1980–2014 in Northern China. *Science of the Total Environment*, **596–597**, 61–68.
Zhang Y B, Liu S Y, Wang J T, Di H J, Han L L, Li P P, Shen J P, Han B, Zhang L M. 2024. The effects and mechanisms of deep straw incorporation and denitrifying bacterial agents on mitigating nitrate leaching and N_2O emissions in four soil types in the North China Plain. *Agriculture*, *Ecosystems & Environment*, **366**, 108958.
Zhao Y, Han X, Qiu C, Zou W, Lu X, Yan J, Chen X. 2025. The enhancements of pore morphology and size distribution by straw return are mediated by increases in aggregate-associated carbon and nitrogen. *Journal of Integrative Agriculture*, **24**, 1562–1576.
Zhao Y, Li P, Liu J, Xiao H, Zhang A, Chen S, Chen J, Liu H, Zhu X, Hussain Q, Wang X, Zhou J, Chen Z. 2025. Microbial effects of prolonged nitrogen fertilization and straw mulching on soil N_2O emissions using metagenomic sequencing. *Agriculture*, *Ecosystems & Environment*, **382**, 109476.
Zhou F, Zhang X, Ma S, Li Y, Zhu M, Zhang W, Li J, Liu X, Hu G, Wang X, He H, Zhang X. 2023. Soil microbial necromass regulation of long-term fertilizer N retention influenced by maize stover mulching. *Geoderma*, **433**, 116453.
Zhu M, Yuan L, Zhou F, Ma S, Zhang W, Miltner A, He H, Zhang X. 2024. Time-dependent regulation of soil aggregates on fertilizer N retention and the influence of straw mulching. *Soil Biology and Biochemistry*, **198**, 109551.

Executive Editor-in-Chief Jinshui Wu
Managing Editor Lujuan Sun